Arch. Metall. Mater., Vol. 61 (2016), No 3, p. 1683–1688

DOI: 10.1515/amm-2016-0274

E. SKOŁEK*,#, K. WASIAK*, W.A. ŚWIĄTNICKI*

THE MICROSTRUCTURE AND PHASE COMPOSITION OF 35CrSiMN5-5-4 STEEL AFTER QUENCHING AND PARTITIONING HEAT TREATMENT

The aim of the study was to characterise the microstructure of 35CrSiMn5-5-4 steel which was subjected to a new heat treatment technology of quenching and partitioning (Q&P). The parameters of the treatment were chosen on the basis of computer simulations and dilatometric studies of phase transformations occurring in steel. The transmission electron microscopy (TEM) observations of steel microstructure after the Q&P treatment revealed the presence of martensite as well as significant amount of retained austenite in form of layers between the martensite laths. The rod-like carbides in the ferritic areas were also observed, which indicates the presence of lower bainite in steel. It was found that the retained austenite content measured by means of TEM was about 28% for partitioning at 400°C and 25% for partitioning at 260°C. These results are in good agreement with the phase composition calculated theoretically as well as those determined experimentally by use of dilatometric tests.

Keywords: quenching and partitioning treatment, astenitic-martensitic microstructure, dilatometric studies, phase composition

1. Introduction

In recent years, a lot of research was dedicated to produce steels with high fraction of retained austenite, which increases the toughness and ductility without deteriorating strength. [1-6] These are for example steels with carbide-free bainite [1, 2, 6] or steels containing martensite and retained austenite enriched with carbon [5, 7]. The efficient heat treatment which allows obtaining in steel the martensitic-austenitic microstructure is called quenching & partitioning (Q&P) [8, 9]. During the "quenching" stage the desired content of martensite is achieved. The second stage – "partitioning" performed at increased temperature is intended to stabilize the remaining austenite. The stabilization of austenite is obtained by enriching it in carbon atoms which escape by diffusion from martensite laths. Metastable austenite content in the steel structure is very advantageous because of the Transformation Induced Plasticity (TRIP) effect [2, 10]. The carbon partitioning occurs during the austempering of steel immediately after the quenching stage. Austempering can be done at the quenching temperature or higher. "Quenching & Partitioning" treatment is applied for steels containing elements that inhibit the precipitation of carbides, such as Si and Al, whereby precipitation processes do not interfere with the partitioning of carbon.

2. Experimental Methods

The 35CrSiMn5-5-4 steel with the chemical composition shown in table 1 was subjected to quenching and partitioning treatment. In order to select the proper parameters of Q&P heat treatment the phase transformations occurring in steel at various temperatures were studied by means of computer simulations and dilatometric tests. The tests were conducted on Bähr 805L quenching dilatometer. The kinetics of phase transformations was evaluated and the characteristic temperatures for steel were determined. The martensite start and finish temperatures were found as: M_s=345°C and M_f=140°C respectively.

The quenching temperature T_Q, which allows obtaining a maximum volume fraction of retained austenite, was calculated by the Magee-Koistinen-Marburger formula [8]:

$$F_{aust.} = e^{((-1.1\times10^{-2})\times(M_S - T_Q))} \quad (1)$$

where $F_{aust.}$ is the maximum amount of retained austenite that it is possible to get in the microstructure after quenching in the T_Q temperature [˚C].

On the basis of above calculations the quenching temperature T_Q = 235˚C was chosen. The samples were held at the quenching temperature for 10 s, in order to stabilise the temperature in the sample and then it was heated to the partitioning stage. Two different values of partitioning temperature were applied: T_P=400°C with t_p=60s and T_P=260°C with t_p=900s. The partitioning temperatures were chosen on the basis on the dilatometric studies and the values of partitioning time were calculated using the formula [11]:

$$t_p = \frac{\bar{x}_a^2}{6\times D_a} + \frac{\bar{x}_m^2}{6\times D_m} \quad (2)$$

where $\bar{x}_a$, $\bar{x}_m$ – average diffusion path of carbon in austenite and martensite respectively

* WARSAW UNIVERSITY OF TECHNOLOGY, FACULTY OF MATERIALS SCIENCE, 141 WOŁOSKA STR., 02-507 WARSAW, POLAND

Corresponding author: emilia.skolek@nanostal.eu

TABLE 1

chemical composition of 35CrSiMn5-5-4, in wt. %.

	C	Mn	Si	Cr	Mo	Ni	V	Al	S	P
35CrSiMn5-5-4	0.36	0.95	1.20	1.30	0.07	0.20	0.03	0.15	0.025	0.035

D_a, D_m - diffusion coefficient of carbon in austenite and martensite respectively

The quenching and partitioning heat treatments were conducted on a laboratory scale in a dilatometer furnace. Cylindrical samples with a diameter of ϕ = 3 mm and height h = 10mm were used. After heat treatment the samples were subjected to the microstructural observations with the use of scanning electron microscope and transmission electron microscope (bright field BF and dark field DF observations) combined with electron diffraction pattern analysis. In order to characterise the microstructure (grain size, content of phases), the methods of stereological analysis were used.

The width of martensite laths and austenite layers visible on the TEM images were determined from the formula:

$$d = \frac{2}{\Pi} L \tag{3}$$

where d is actual width of the microstructure element, L – the width of this element measured on TEM image [12].

Volume fraction of each phase was calculated with the assumption that it is equivalent to its surface fraction area in the microstructure image plane. A number of secant lines of the length *l* was applied to images of microstructure intersecting with specific phase n-times. The following formula was used to calculate the phase content:

$$V_v = \frac{\Sigma c_{ik}}{l} \tag{4}$$

where $\sum c_{ik}$ is the sum of the widths of all intersections of the secant line l with a given phase, l – length of the secant line.

The results of calculations were compared with the results of the analyses of dilatograms. This made it possible to examine the effect of temperature and time of partitioning on the content of retained austenite in the microstructure

3. Results and discussion

According to the literature, the final austenite fraction is strongly dependend on quenching and partitioning parameters [8, 9, 11, 13, 14] and is different than the theoretically calculated level [8, 9, 11, 13, 14]. In the present work it was decided to produce a structure containing ca. 20% of retained austenite. Fig. 1 shows a comparison of changes in the content of retained austenite as a function of quenching temperature, calculated according to the formula (1) and determined on the basis of performed dilatometric tests. On the basis of the dilatometric studies the amount of retained austenite for various temperatures was designated graphically from the change in length – temperature curve. Further the carbon content in the retained austenite after quenching stage in various temperatures was calculated. Furthermore new Ms temperatures was determined and the final austenite content after Q&P process for various temperatures of quenching stage was calculated from eq. 1. The calculated values were plotted and compared with theoretical calculations. Quenching temperature for maximum content of stable austenite (ca. 35%) at the temperature of 250˚C, is almost identical for both, the theoretical calculations and the experimental determination by dilatometric study. However, if the temperature of quenching moves away from the temperature value corresponding to a maximum austenite content the calculated volume fraction of austenite differs from that determined from dilatograms. In study, the quenching temperature was selected on the basis of dilatometric tests which indicated that the 20% of retained austenite volume fraction can be obtained by quenching at a temperature of 235 °C (Fig. 1).

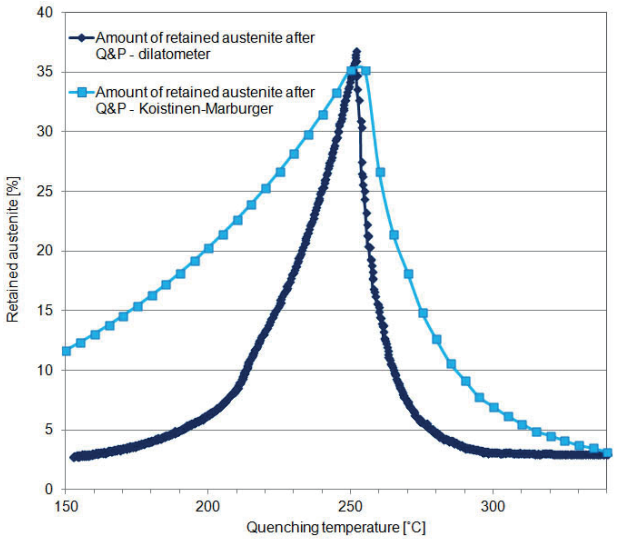

Fig. 1. Changes in the content of the retained austenite based on quenching treatment temperature

Fig. 2 presents the time of partitioning stage as a function of temperature, calculated using the formula (2), providing stabilization of retained austenite at given conditions. In this work two partitioning temperatures were applied: the frequently used 400 °C and much lower temperature: 260° C, for which the carbon partitioning takes much longer time. Both designed processes of quenching and partitioning should in principle ensure to obtain approximately 20% of stable retained austenite. The parameters of both Q&T heat treatments are presented in Table 2.

TABLE 2

Parameters of the quenching and partitioning treatments

Symbol of heat treatment	Quenching temperature T_Q [°C]	Partitioning temperature T_P [°C]	Partitioning time t_P [s]
Q&P400	235	400	60
Q&P260	235	260	900

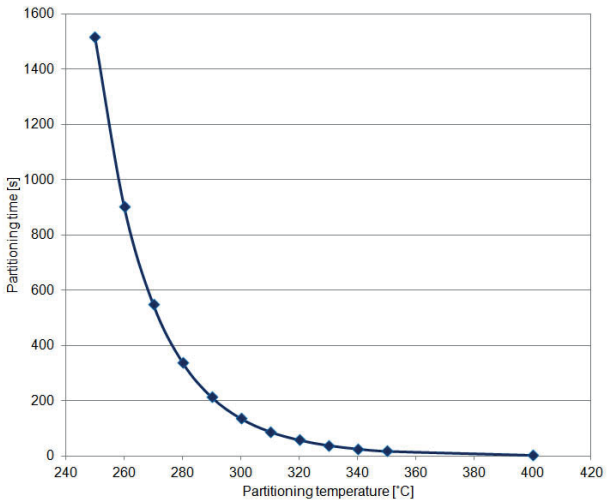

Fig. 2. Time-temperature relationship for the partitioning treatment

Observations made with the use of SEM revealed that the microstructure after both Q&T treatments led to a similar microstructure. It was composed of laths of martensite separated by the layers of retained austenite (Fig. 3-4). In some laths of martensite carbide precipitates were observed. The microstructure of samples after Q&P260 heat treatment is less fragmented compared to the microstructure of the microstructure of samples after Q&P400.

Detailed observations carreid out with the use of TEM confirmed the presence of martensite laths in the microstructure, as well as occurrence of elongated carbide precipitates in the ferrite areas. This indicates that the microstructure is composed of a mixture of tempered martensite and lower bainite. Small amount of carbides precipitations between laths of martensite and layers of austenite was also observed. The bainitic structure could be formed during the partitioning stage, as a result of decomposition of residual austenite [15, 16]. The presence of cementite precipitates in martensite and in bainitic ferrite indicates that the concentration of elements Si+Al in steel is insufficient to completely inhibit the precipitation of carbides during heat treatment. The average width of martensite laths was 175 ± 21 nm and 217 ±26 nm in sample after heat treatments Q&P400 and Q&P260 respectively. Moreover in the microstructure of steel after quenching at 235˚C and partitioning at 260 ˚C for longer time (900 s), a smaller amount of ferrite laths with a thickness below 200 nm compared to the

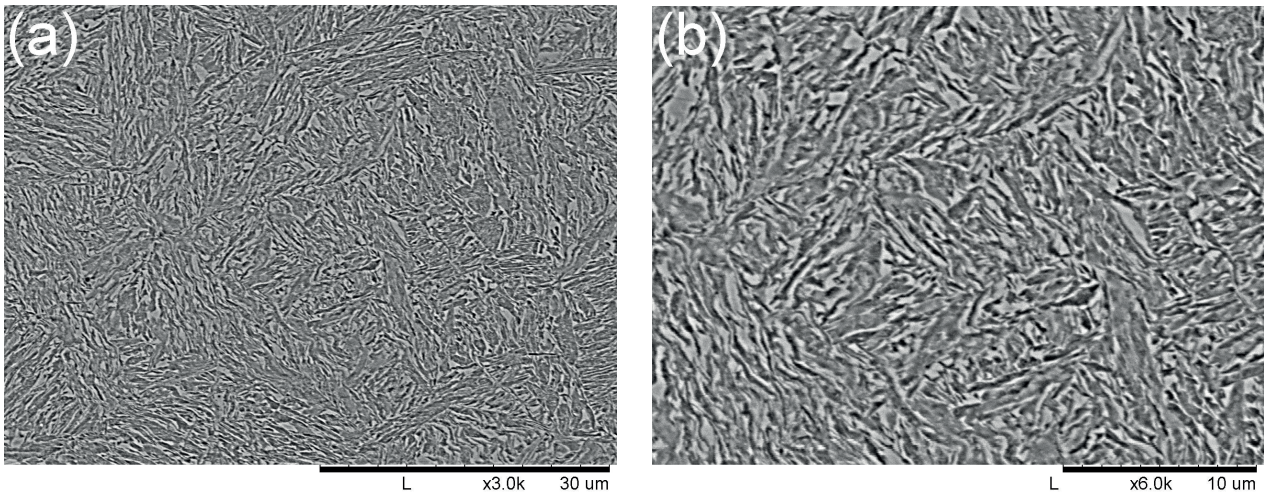

Fig. 3. Microstructure of 35CrSiMn5-5-4 steel after quenching at 235 ˚C and partitioning at 400 ˚C for 60 s

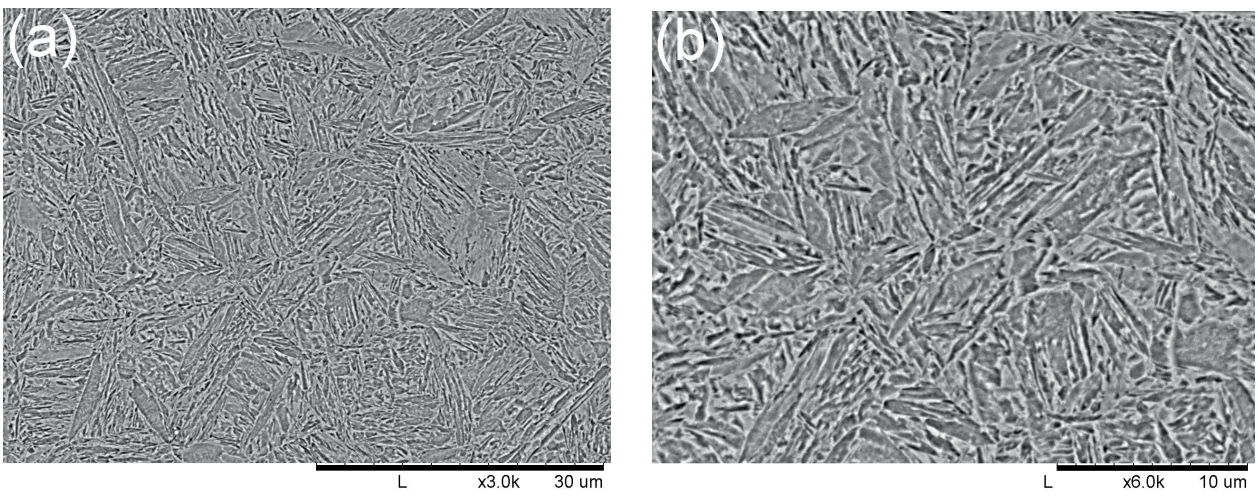

Fig. 4. Microstructure of 35CrSiMn5-5-4 steel after quenching at 235 ˚C and partitioning at 260 ˚C for 900 s

quenching at 235˚C and partitioning at 400˚C for shorter time (60 s) was observed (fig. 9a). Therefore it can be concluded, that a longer treatment time causes the growth of ferrite laths – similar phenomenon was also observed by other authors [15]. Between bainite/martensite laths the layers of retained austenite with the average value of 55 ± 6 nm after Q&P400 and of 50 ± 6 nm Q&P260 were observed (fig. 5-8). In case of the retained austenite layers, longer time of the Q&P treatment leads to decrease of the retained austenite layers' thickness – higher amount of the retained austenite layers with the thickness below 100 nm in the microstructure of the Q&P260 was observed (fig. 9b). In both cases dislocation loops in the martensite were found. The austenite content measured on the microscopic images is approximately equal

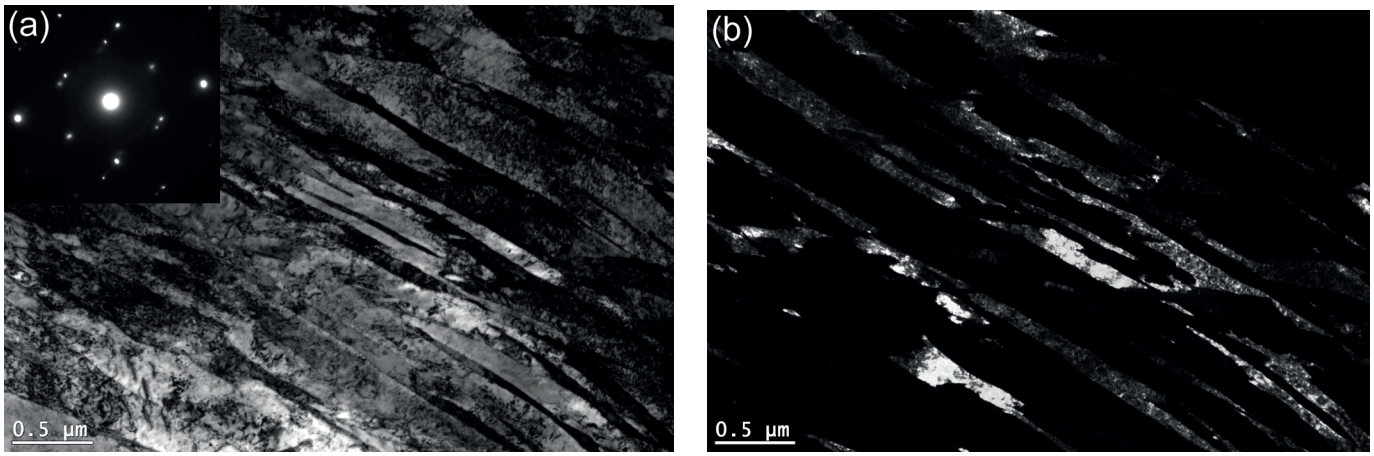

Fig. 5. Microstructure of 35CrSiMn5-5-4 steel after quenching at 235 ˚C and partitioning at 400 ˚C for 60 s (a) – bright field image, (b) – dark field image for austenite reflection

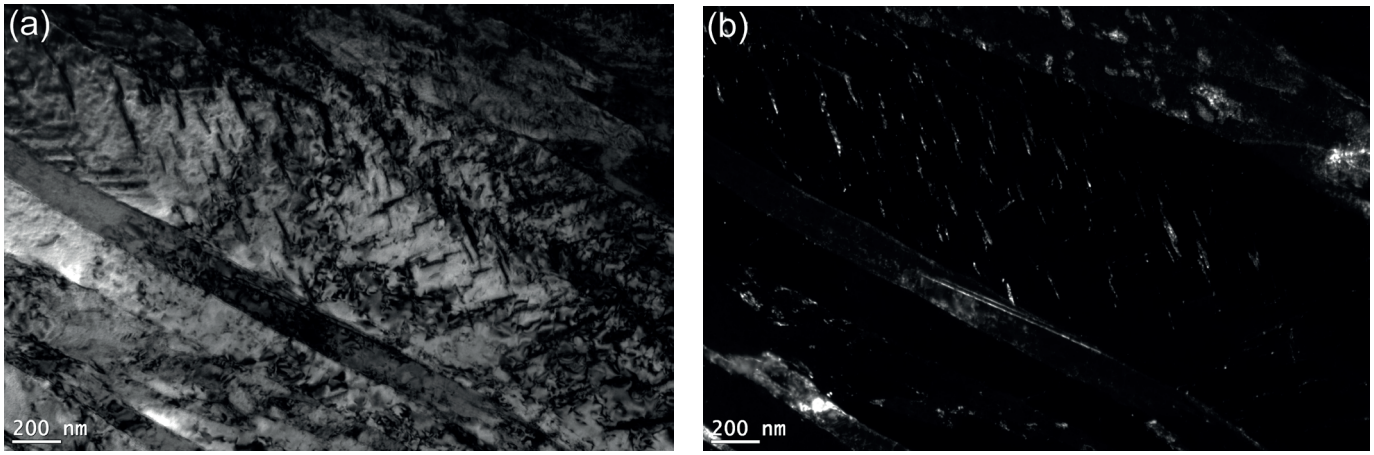

Fig. 6. Microstructure of steel sample after quenching at 235˚C and partitioning at 400˚C for 60 s, (a) – bright field image, (b) – dark field image for cementite reflection

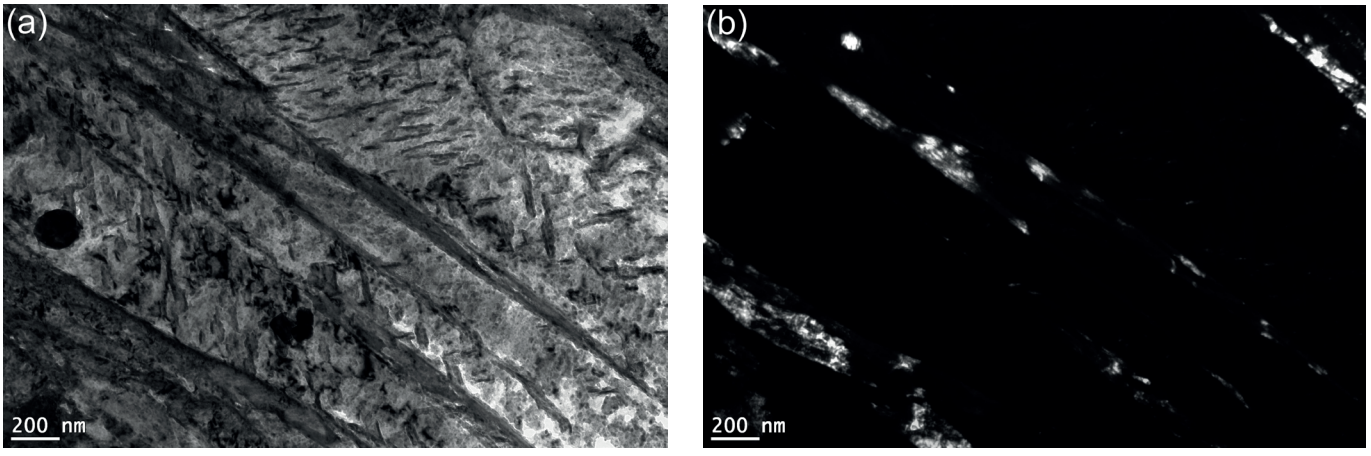

Fig. 7. Microstructure of steel sample after quenching at 235˚C and partitioning at 260 ˚C for 900 s, (a) – bright field image, (b) – dark field image for austenite reflection

to 28 % ± 5 % and 25 % ± 5 % after Q&P400 and Q&P260 respectively. These values are similar to those estimated from the dilatograms. After both heat treatments, the twinned martensite without carbides were also found (fig. 8). These laths of "fresh", martensite could be formed during final cooling of a sample to room temperature. It indicates, that the enrichment of the austenite during partitioning stage may be not uniform in the microstructure, and thus some unstable austenite may remain after partitioning and transforms to martensite during final cooling.

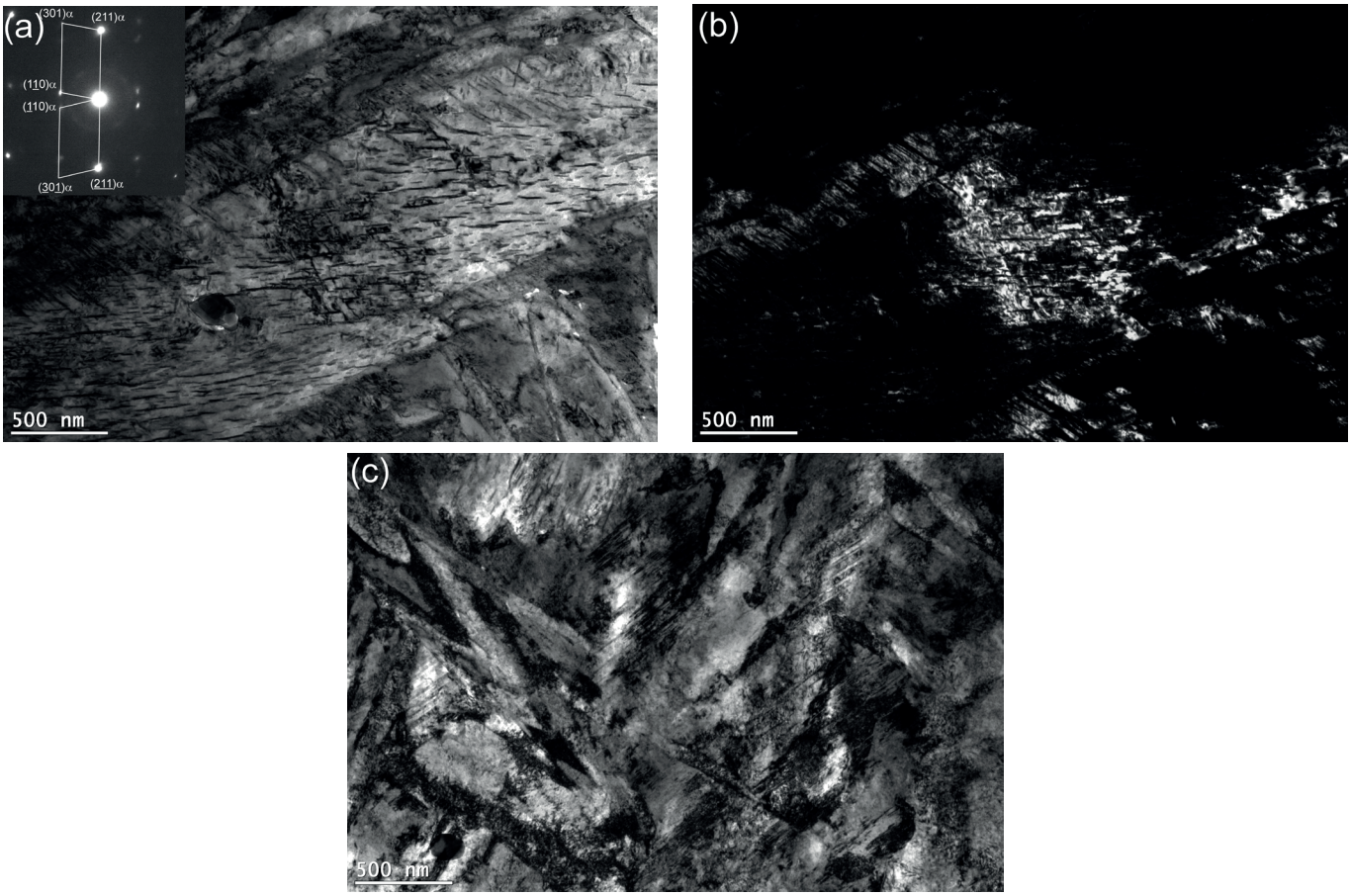

Fig. 8. Microstructure of 35CrSiMn5-5-4 steel after quenching at 235 ˚C and partitioning at 260 ˚C for 900 s (a), (c) – bright field image, (b) – dark field image for ferrite reflection

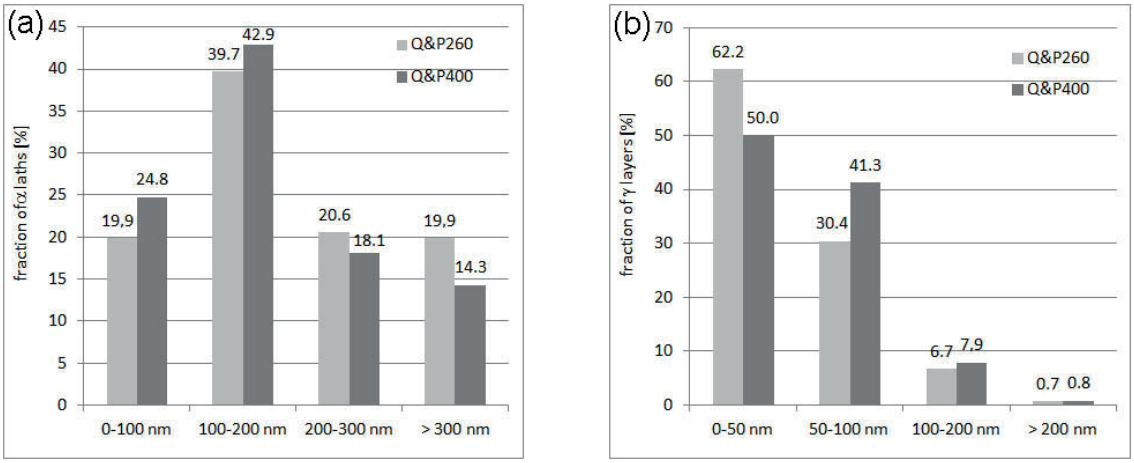

Fig. 9. Distribution of size of ferrite laths and retained austenite layers in the microstructure of 35CrSiMn5-5-4 steel after quenching at 235 ˚C and partitioning at 260 ˚C for 900 s (a) and after quenching at 235˚C and partitioning at 400˚C for 60 s (b)

4. Summary:

The application of a quenching and partitioning heat treatment to 35CrSiMn5-5-4 steel leads to a microstructure consisting mostly of martensite laths surrounded by retained austenite layers. The rod-like carbides in the ferritic areas were also observed, which indicates the presence of a lower bainite in the microstructure. The microscopic observations carried out with the SEM and TEM did not reveal the significant differences between the microstructures produced with the use of various parameters of quenching and partitioning treatment, except for the size of the microstructure elements. Amount of retained austenite evaluated with the use of microscopic observations is about 28% for partitioning at 400°C and 25% for partitioning at 260°C and it is similar to the theoretical calculations and the results obtained by dilatometric tests.

Acknowledgements

The results presented in this paper have been obtained within the project "Production of nanocrystalline steels using phase transformations" – NANOSTAL (contract no. POIG 01.01.02-14-100/09 with the Polish Ministry of Science and Higher Education). The project is co-financed by the European Union from the European Regional Development Fund within Operational Programme Innovative Economy 2007-2013.

REFERENCES

[1] A. Grajcar, R. Kuziak, W. Zalecki, Archives of Civiland Mechanical Engineering **12,** 334 (2012).

[2] A. Grajcar, Archives of Materials Science and Engineering **33**, 5 (2008).

[3] A. Kokosza, J. Pacyna, Archives of Materials Science and Engineering **31**, 87 (2008).

[4] A. Grajcar, W. Kwaśny, Journal of Achievements in Materials and Manufacturing Engineering **54**, 168 (2012).

[5] A. Grajcar, H. Krztoń, Journal of Achievements in Materials and Manufacturing Engineering **35**, 169 (2009).

[6] C. Garcia-Mateo, F.G. Caballero, Materials Transactions **46**, 1839 (2005).

[7] J. Speer, D.K. Matlock, B.C. De Cooman, J. G. Schroth, Acta Materialia **51**, 2611 (2003).

[8] A.J. Clarke, J.G. Speer, M.K. Miller, R.E. Hackenberg, D.V. Edmonds, D.K. Matlock, F.C. Rizzo, K.D. Clarke, E. De Moor, Acta Materialia **56**, 16 (2008).

[9] J.G. Speer, D.V. Edmonds, F.C. Rizzo, D.K. Matlock, Current Opinion in Solid State and Materials Science **8**, 219 (2004).

[10] A. Kokosza, J. Pacyna, Archives of Metallurgy and Materials 55, 1001(2010).

[11] H.Y. Li, X.W. Lu, X.C. Wu, Y.A. Min, X.J. Jin, Materials Science and Engineering: *A,* 527, 6255 (2010)

[12] L.C. Chang, H.K.D.H. Bhadeshia, Materials Science and Technology **11**, 874 (1995).

[13] D.V. Edmonds, K. He, F.C. Rizzo, B.C. De Cooman, D.K. Matlock, J.G. Speer, Materials Science and Engineering A, **438-440**, 25 (2006).

[14] E. Paravicini Bagliani, M. J. Santofimia, L. Zhao, J. Sietsma, E. Anelli, Materials Science & Engineering A **559**, 486 (2013).

[15] X. Tan,Y. Xu, X. Yang, Z. Liu, D. Wu, Materials Science&Engineering A **594**, 149 (2014).

[16] M. J. Santofimia, L. Zhao, J. Sietsma, Metallurgical and Materials Transactions A **40A**, 46 (2009).